JOURNAL OF GEOPHYSICAL RESEARCH, VOL. 106, NO. D9, PAGES 10,023–10,038, MAY 16, 2001

Isentropic scaling analysis of ozone in the upper troposphere and lower stratosphere

John Y. N. Cho, Valérie Thouret,[1] and Reginald E. Newell
Department of Earth, Atmospheric, and Planetary Sciences
Massachusetts Institute of Technology, Cambridge, Massachusetts

Alain Marenco
Laboratoire d'Aérologie, Centre National de la Recherche Scientifique
Observatoire Midi-Pyrénées, Université Paul Sabatier, Toulouse, France

Abstract. We examine ozone concentrations recorded by 7630 commercial flights from August 1994 to December 1997 for spatial scaling properties. The large amount of data allows an approximately isentropic analysis of ozone variability in the upper troposphere and lower stratosphere. Since ozone is a good passive tracer at cruise altitudes, the results provide a strong diagnostic for scalar advection theories and models. Calculations of structure functions and increment probability distribution functions show that ozone variability scales anomalously from ~2 to ~2000 km, although not continuously in this interval. We find no evidence for the simple scaling predicted for smooth advection/diffusion, even at the large scales. At mesoscales the upper tropospheric ozone field is rougher and more intermittent than in the lower stratosphere. Within the troposphere the equatorial ozone field is rougher than at higher latitudes, and the intermittency decreases with increasing latitude. In the stratosphere the intermittency and roughness are greater at high latitudes and over land than at midlatitudes and over the ocean.

1. Introduction

Ozone is an important trace gas in both the stratosphere and the troposphere. In the former region it filters harmful solar ultraviolet rays, while in the latter region it can add to the greenhouse effect on one hand and regulate the air's oxidizing (cleansing) capacity on the other hand. At the surface, an overabundance of ozone is dangerous to many organisms.

Thus there is a great deal of interest in modeling atmospheric ozone distribution on both regional and global scales. Clearly, both chemistry and transport processes must be properly incorporated into such models in order to adequately mimic the real world. However, at 9–12 km altitude the chemical lifetime of ozone is at least 100 days, according to *Wang et al.* [1998], so the spatial variability should be mainly generated dynamically. Other references give somewhat shorter lifetimes [e.g., *Brasseur et al.*, 1999], but comparison of mesoscale ozone fluctuation spectra with those of other even longer-lived species such as nitrous oxide, methane, and carbon dioxide shows that they are very similar in form [*Bacmeister et al.*, 1996; *Cho et al.*, 1999c]. Therefore the ozone variability at these altitudes ought to be a strong diagnostic for passive scalar transport models and theories.

Earlier work usually used the Fourier power spectrum as the arena for comparison between theory and observation. The results have not been conclusive. *Nastrom et al.* [1986] calculated ozone power spectra for 10–2400 km wavelengths using data collected at cruising altitude by specially equipped commercial aircraft. Their results showed log-log spectral slopes of approximately −5/4 for 500–2400 km wavelengths, approximately −5/3 for shorter wavelengths in the lower stratosphere (LS) and for 100–500 km wavelengths in the upper troposphere (UT), and approximately −1 for scales < 100 km in the UT. The corresponding horizontal velocity power spectra for combined UT/LS data had slopes of approximately −3 for scales longer than ~400 km and approximately −5/3 for shorter scales [*Nastrom and Gage*, 1985]. Their interpretation for the coincident −5/3 mesoscale spectra was inverse-energy-cascade stratified turbulence [*Gage*, 1979; *Lilly*, 1983, 1989] and quasi-horizontal advection acting against the vertical gradients of the scalars [*Gage and Nastrom*, 1986]. The −5/4 slope of ozone

[1]Now at the Laboratoire d'Aérologie, Centre National de la Recherche Scientifique, Observatoire Midi-Pyrénées, Université Paul Sabatier, Toulouse, France.

Paper number 2000JD900733.
0148-0227/01/2000JD900733$09.00

at longer scales did not quite match the -1 slope predicted for enstrophy-cascade two-dimensional (2-D) turbulence [*Fasham*, 1978; *Lesieur et al.*, 1981], while the -1 slope at small scales was a complete mystery.

More recent studies using high-quality (but limited quantity) research aircraft data have yielded a uniform $-5/3$ slope for ozone power spectra at 1–100 km scales in the middle stratosphere [*Bacmeister et al.*, 1996] and in the free troposphere [*Cho et al.*, 1999c]. In the former study a gravity wave explanation [*Dewan*, 1979; *VanZandt*, 1982; *Gardner et al.*, 1993] was favored because the horizontal velocity spectra broke from a slope of $-5/3$ to -3 at scales < 3 km; however, simple wave advection across scalar gradients could not account for the discrepancy in spectral form between velocity and ozone. In the latter study the similarity of spectral form for velocity and ozone allowed either the turbulence or wave explanation.

Realizing the ambiguities of employing solely power spectral techniques, other methods were introduced to this problem [*Bacmeister et al.*, 1997; *Cho et al.*, 1999a; *Lindborg*, 1999; *Tuck and Hovde*, 1999]. For example, intermittency is a quality not characterized by power spectra. Note that both white noise and randomly distributed Dirac delta functions yield a flat power spectrum, even though they are radically different in intermittency. Also, real-life data with uneven sampling and gaps present problems for Fourier spectral analysis, and one must be concerned with power leakage that can alter spectral forms, especially for "red noise" characteristic of most geophysical data [e.g., *Dewan and Grossbard*, 2000]. For all of these reasons we will calculate structure functions and increment probability distribution functions (PDFs) in this study. The results will be compared to both the power spectral analyses of the past and to recent theoretical and modeling work involving scaling and fractal formalisms.

The structure function and increment PDF approach to scalar field characterization that we have chosen derive from turbulence studies [e.g., *Frisch*, 1995; *Shraiman and Siggia*, 2000]. Others have taken the more geometric route of fractal scaling via measures such as the Kolmogorov capacity [*Methven and Hoskins*, 1998] or the Hurst exponent [*Tuck and Hovde*, 1999], which are related to each other [*Vassilicos and Hunt*, 1991]. There are pros and cons for every method. We chose our particular approach mainly for the ease with which the results could be parsed with respect to ozone, potential temperature, and latitude values. Also, by calculating higher-order structure functions we were able to obtain two scaling parameters (relating to roughness and intermittency), thus providing more information than single-exponent methods.

2. Data

A very large collection of UT/LS in situ ozone data is available through the measurement of ozone and water vapor by Airbus in-service aircraft (MOZAIC) program [*Marenco et al.*, 1998]. Five Airbus A340 aircraft have been regularly measuring ozone, humidity, horizontal wind, and temperature since August 1994 (see *Cho et al.* [1999b] for a schematic of flight routes). The sampling interval is 4 s, while the response time of the ozone instrument is 8 s (see *Marenco* [1996] for further details). For a nominal cruising speed of 250 m s^{-1} this corresponds to an effective horizontal resolution of 2 km for ozone. The humidity sensor has a response time that increases with decreasing temperature (from below 10 s near the ground to as long as 3 min at 12-km altitude) [*Helten et al.*, 1998]; therefore it is not very suitable for scaling analyses. Structure function analyses of the horizontal winds have been performed previously [*Lindborg*, 1999; *Cho and Lindborg*, 2001; *Lindborg and Cho*, 2001]. The cascade of passive scalar variance in the lower stratosphere was also measured from the third-order structure functions [*Lindborg and Cho*, 2000].

We used data from 7630 flights (August 1994 to December 1997). The distances between two data points were calculated using the latitude, longitude, and altitude information, and the distance was taken to be the shortest arc length along a spherical surface rather than the straight line. Note that the latitude-longitude coordinates for the Air France aircraft data were purposely degraded to 1-min resolution (a result of pilot union concerns), so we linearly interpolated the position to the original 4-s sampling intervals. Since sharp turns were almost never performed at cruising altitude, the differences introduced by this procedure should be negligible. The position data from the other airlines (Sabena, Lufthansa, and Austrian Airlines) were archived at the original sampling rate.

The ozone values themselves were used to differentiate between UT and LS. If the ozone levels associated with the pair of data points were both under 100 ppbv, then the result was binned as tropospheric. If the ozone concentrations for both members of the data point pair were over 200 ppbv, then the result was classified as stratospheric. If one point was in the troposphere and the other point was in the stratosphere, the result was not included in either group. Latitudinal dependence was studied by parsing the data point pairs into four bands: 0°–10°, 10°–30°, 30°–50°, and 50°–70°, where the value used was the absolute value of the average of the latitudes at the two points. We also subdivided the flights into oceanic and overland categories. Oceanic flights went between western Europe and the eastern seaboard of North America, the Caribbean, or the northeast coast of South America. Overland flights were between Europe and Africa, the Middle East, or Asia, excluding flights that went over the Indian Ocean.

There were five standard flight levels from 9.4 to 11.8 km, each spaced 600 m apart. The adherence to the standard levels was quite strict [*Thouret et al.*, 1998]. For the purposes of scalar advection, however, constant potential temperature (θ) surfaces are more relevant. Therefore we restricted our calculations to data point pairs that were approximately isentropic, i.e., a θ differ-

ence of < 1 K. Finer binning was not chosen, because although the precision of the temperature measurement was smaller, the accuracy was estimated to be of the order of 1 K. We did try the computations using θ bins as small as 0.1 K, and the resulting forms of the structure functions were similar to the 1 K case. Of course, isentropic transport is only an idealization, even at large scales in the stratosphere [*Sparling et al.*, 1997].

3. Structure Functions

Computation of structure functions is straightforward, and data gaps are easily handled (unlike with Fourier spectral methods). They are defined as

$$S_q(r) = \langle |\chi(x+r) - \chi(x)|^q \rangle \ , \tag{1}$$

where $\chi(x)$ is a one-dimensional signal (in our case the time series of ozone mixing ratio), r is some finite difference in x, angle brackets denote an ensemble average, and q is the order of the structure function. In turbulence literature, S_2 is often called "the" structure function, but we will follow the convention that S_q of any order is a structure function. We choose to compute $S_q(r)$ for $r = 1$, 2, 4, 8, 16, 32, 64, 128, 256, 512, 1024, 2048, and 4096 km and q in integer increments. For each data point at x the rest of the flight (going forward in time) is searched for the points that come closest to $x + r$ for every specified r value. The calculation proceeds if the difference between the actual distance and the specified r is < 0.5 km and the other data acceptance criteria (as explained in section 2) are met. Note that Taylor's frozen turbulence hypothesis is implicit in this calculation, an assumption that may be questionable for advective timescales at $r \gtrsim 1000$ km [*Lindborg*, 1999].

If $S_q(r)$ displays straight-line intervals on a log-log plot, we can investigate how the qth-order structure function scales with r. In other words, we can derive the exponent ζ_q in

$$S_q(r) \propto r^{\zeta_q} \ . \tag{2}$$

We know a few general things about ζ_q: $\zeta_0 = 0$ by definition, ζ_q is concave ($d^2\zeta_q/dq^2 < 0$) [*Davis et al.*, 1994], and if $\chi(x)$ is bounded, then ζ_q is monotonically nondecreasing [*Frisch*, 1991]. If ζ_q/q is a constant, then the relation is called simple scaling, while a variable ζ_q/q denotes anomalous scaling. (Anomalous scaling has been argued to be equivalent to multifractality of the measured structure [*Pierrehumbert*, 1994; *Vainshtein et al.*, 1994].)

If ζ_q exhibits simple scaling, then it does not give us more information about the signal than the Fourier power spectrum, since S_2 is in Fourier duality with the power spectrum for nonstationary processes with stationary increments. However, if ζ_q shows anomalous scaling, then it will contain information not provided by the power spectrum, i.e., the degree of intermittency.

There are a limited number of analytical expressions for ζ_q available from passive scalar mixing theory with which we can compare our results. Chaotic isentropic advection by a smooth velocity field (including diffusion) has been predicted to yield simple scaling [*Pierrehumbert*, 1994; *Chertkov et al.*, 1995; *Antonsen et al.*, 1996], with

$$S_q(r) \propto [\ln(r/r_0)]^{\zeta_q} \ , \tag{3}$$

where r_0 is a diffusive inner scale and $\zeta_q = q/2$ [e.g., *Pierrehumbert*, 2000]. This type of smooth advection corresponds to the Batchelor regime in the Fourier power spectral domain where the log-log slope is -1 [*Batchelor*, 1959]. For advection/diffusion by a random Gaussian velocity field δ correlated in time with self-similar correlations in space, *Kraichnan* [1994] predicted anomalous scaling of the form

$$\zeta_q = \frac{1}{2}\left[2qd\zeta_2 + (d-\zeta_2)^2\right]^{\frac{1}{2}} - \frac{1}{2}(d-\zeta_2) \ , \tag{4}$$

where d is the spatial dimension. The $q^{1/2}$ behavior at large q has been disputed by other studies that suggest a saturation of ζ_q at a constant value [*Chertkov*, 1997; *Balkovsky and Lebedev*, 1998]. Bounded multiplicative random cascade models also show saturation [*Marshak et al.*, 1994]. In another development, *Cao and Chen* [1997] utilized a three-dimensional (3-D) passive-scalar turbulence scheme based on a bivariate log-Poisson model and derived

$$\zeta_q = 3 - \frac{q}{36} - 2\left(\frac{3}{4}\right)^{\frac{q}{6}} - \left(\frac{1}{2}\right)^{\frac{q}{2}} + \gamma\left[1 - \left(\frac{3}{4}\right)^{\frac{q}{6}} - \left(\frac{1}{2}\right)^{\frac{q}{2}} + \left(\frac{3}{4}\right)^{\frac{q}{6}}\left(\frac{1}{2}\right)^{\frac{q}{2}}\right] , \tag{5}$$

where γ is an undetermined fitting parameter.

For anomalous scaling, different methods have been proposed to compactly parameterize the calculated ζ_q curves. *Davis et al.* [1997] advocated the use of a bifractal plane with ζ_1 (global Hölder exponent or Hausdorff measure) to characterize the smoothness of the data and an intermittency parameter calculated from singular measures. *Tessier et al.* [1993] proposed a "universal multifractal" parameterization based on three exponents. *Pierrehumbert* [1996] introduced a two-parameter fit

$$\zeta_q = \frac{aq}{1 + a\frac{q}{\zeta_\infty}} \tag{6}$$

to the ζ_q curves, where a measures smoothness (most probable continuity exponent) and ζ_∞ measures multifractality (infinity for monofractality; decreasing with increasing multifractality). Although the two-parameter bifractal plane scheme is attractive, since it requires only first-order quantities that range between 0 and 1, the computation of singular measures requires continuous data and resolution down to the diffusive cutoff, which we do not have. It is possible to obtain

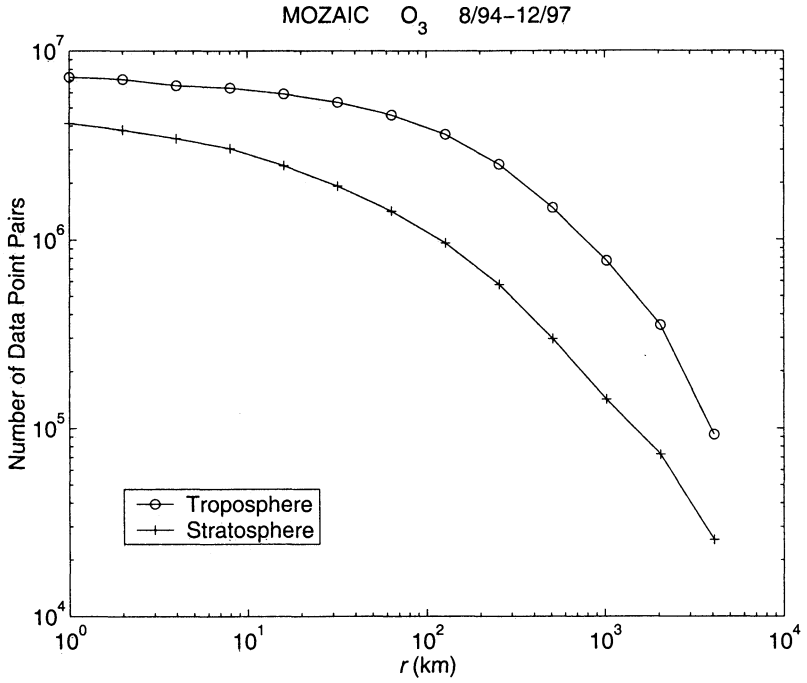

Figure 1. Number of data point pairs used in the calculation of structure functions and increment PDFs.

the first-order singularity exponent from structure functions by assuming a certain physical model [*Davis et al.*, 1997], but it is not possible for the general case. Since (6) can be calculated solely from structure functions, we will adopt it for our study. The bifractal parameters can be also computed from a and ζ_∞ using equation (18) of *Davis et al.* [1999], although the results are not expected to be truly equivalent to those calculated from the first-order exponents of structure functions and singular measures, since the former uses the full q hierarchy, whereas the latter relies only on $q = 1$ quantities.

Figure 1 shows the number of data point pairs used in computing the structure functions. As expected for finite length flight segments, the number of data pairs fell off with increasing r. There were well over a million pairs available at the shorter scales, and even at the longest scale, there were well over 10,000 pairs. Note that there were fewer data points in the LS than in the UT.

Figure 2 shows the calculated structure functions for UT data, with $q = 1$ to 5 (bottom to top). Note that scaling was quite good throughout at mesoscales. Even for $q > 5$, the scaling was good in this regime for extratropical data, and the log-log slopes saturated close to the $q = 5$ value. The scaling was generally poorer for tropical data, with the structure functions showing a bit of a dip in the subrange $r \sim 10$–100 km. The drop in amplitude at the shortest scale ($r = 1$ km) was observed in all data, and we attribute this to an instrumental response time (8 s) that was slower than the sampling interval of 4 s. This interpretation is consistent with past aircraft experiments using ozone probes with faster response times (0.5–1 s) that did not yield a spectral break at these scales [*Cho et al.*, 1999c]. At $r \gtrsim 500$ km the structure functions began to curve slightly downward (except for the final points at $r = 4096$ km).

Via the Wiener-Khinchine relation that connects the second-order structure function with the Fourier power spectrum, we can obtain $\beta = \zeta_2 + 1$, where β is the negative exponent of the horizontal wave number power spectrum. This relationship is valid for $1 < \beta < 3$ (nonstationary signal with stationary increments) [e.g., *Frisch*, 1995], a criterion that was satisfied in this case. Note that β in this subrange was almost exactly 5/3, which is consistent with recent tropospheric results [*Cho et al.*, 1999c].

An attempt to fit these structure functions at all ranges by the logarithmic function (3) failed. It is clear that power law scaling is appropriate at mesoscales. Therefore we fit straight lines in a least squares sense to the functions for $r = 2$–256 km (the exact choice of the upper endpoint is, admittedly, somewhat arbitrary), then plotted the slopes (ζ_q) in Figure 3. In Figure 3 we have plotted a curve that corresponds to simple scaling (solid curve), a plot of (4) with $d = 2$ (dot-dashed curve), a fit of (5) (dotted curve) with the fitted γ value displayed, and a fit of (6) (dashed curve) with the derived a and ζ_∞ shown. For convenience, ζ_1 is also printed.

The scaling was clearly anomalous and the computed ζ_q values were more multifractal than either the Kraichnan 2-D or Cao-Chen model. (Higher-dimensional Kraichnan curves are less multifractal than the 2-D curve.) The smoothness parameter, ζ_1, was 0.35, which

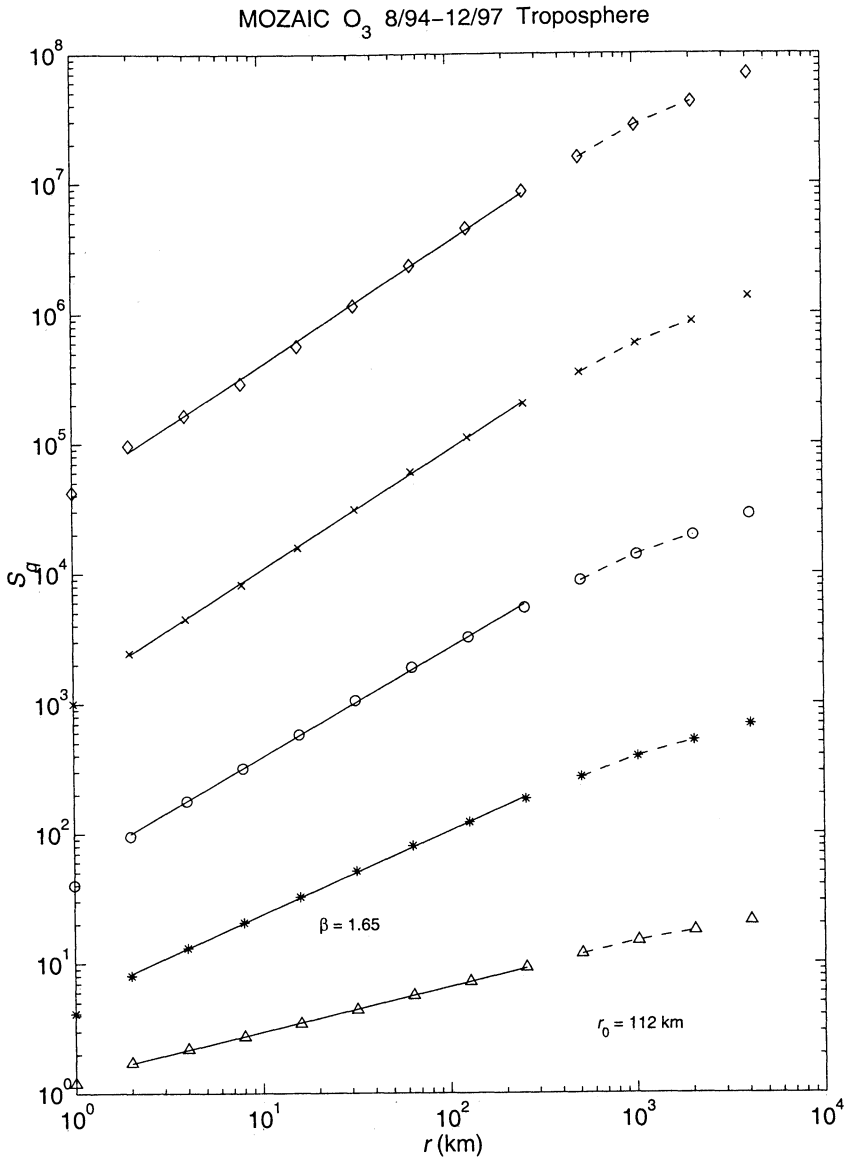

Figure 2. Calculated ozone structure functions for the upper troposphere, with $q = 1$–5. The order increases in unity steps from bottom to top. Units are in $(\text{ppbv})^q$. Power law fits are shown as solid curves, and logarithmic fits are displayed as dashed curves.

is rougher than standard Brownian motion ($\zeta_1 = 0.5$) but smoother than white noise ($\zeta_1 = 0$). (Almost everywhere differentiable functions yield $\zeta_1 = 1$.)

At longer scales we tried to fit (3) to a limited subrange ($r = 512$–2048 km). First, we let r_0 be a free parameter and fit S_2 with $\zeta_q = 1$. Then, using the derived r_0 (shown in Figure 2), we fit the data (dashed curves in Figure 2) by varying ζ_q, which are plotted in Figure 4. By choosing to fit S_2 first (an arbitrary choice), ζ_2 is constrained to be close to 1, but the point of the exercise was to investigate whether ζ_q would exhibit simple scaling as expected for the Batchelor smooth advection/diffusion regime. We see that even at these large scales, UT ozone variability scaled anomalously. The scaling itself, however, must be questioned because of its short range. It is also possible that at the longest scales the results may suffer from a breakdown of Taylor's hypothesis.

Structure functions for LS data are shown in Figure 5. Scaling broke down more rapidly with q compared to the UT data, so we performed the fits only up to $q = 4$. The functions also appeared to curve downward at shorter scales compared to the UT case, so we adjusted the fitting subranges accordingly. Note that β was significantly larger than for the UT case and cannot be said to be close to 5/3. The result of the fits are displayed in Figures 4 and 6. Again, the results were multifractal but less so (less intermittent) than for the UT data. The Cao-Chen model fit poorly, but the Kraichnan 2-D model did well up to $q = 3$. (The Cao-Chen fit is worse than it looks because we let γ be any value, whereas realistically it should probably not ex-

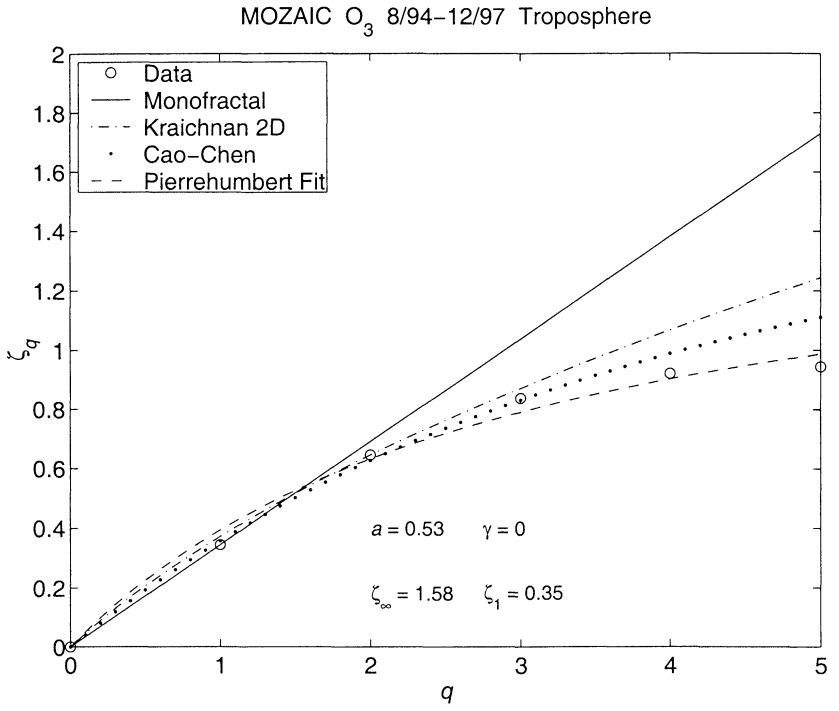

Figure 3. Plot of ζ_q calculated from the solid curves shown in Figure 2 (circles). Other functions are also plotted as indicated in the legend. See text for further details.

ceed 1.) The $\zeta_1 = 0.5$ indicates a smoother ozone field than in the UT and is comparable to Hurst exponents for LS ozone fluctuations compiled by *Tuck et al.* [1999]. (The exponent ζ_1 of a signal is equivalent to the Hurst exponent of the first differences of the signal for a self-affine signal (A. Tuck, personal communication, 2000).) The large-scale fits to (3) also did not support simple scaling.

We also calculated results for data taken at latitudes 50°N–70°N during June–July versus December–January, i.e., during the period of shortest versus longest chemical lifetime for ozone. The invariance of ζ_1

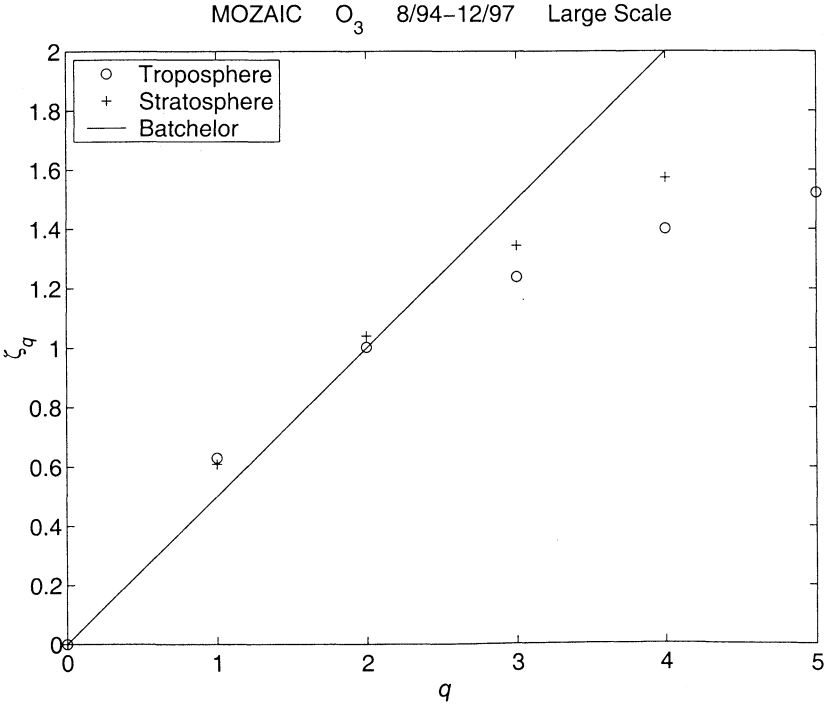

Figure 4. Plot of ζ_q calculated from the dashed curves shown in Figure 2 (circles), and plot of ζ_q calculated from the dashed curves shown in Figure 5 (crosses).

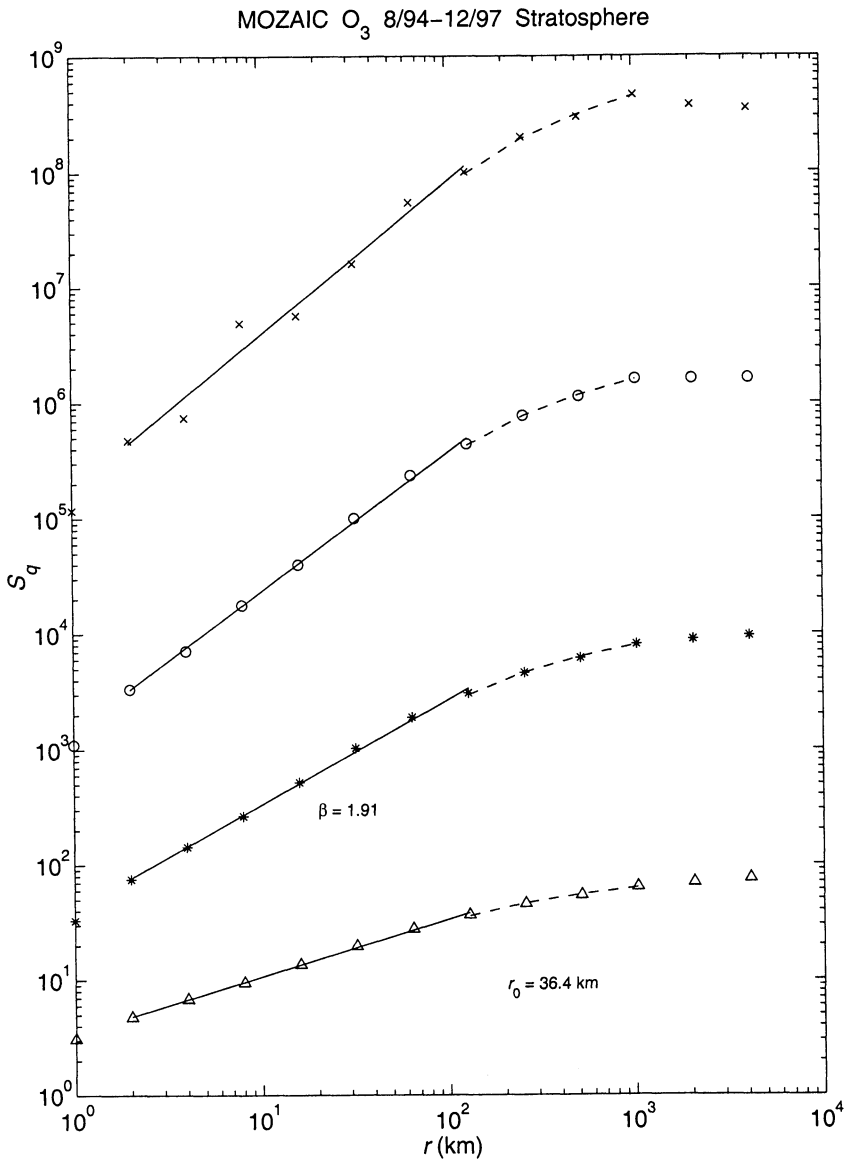

Figure 5. Calculated ozone structure functions for the lower stratosphere, with $q = 1$–4. The order increases in unity steps from bottom to top. Units are in $(\text{ppbv})^q$. Power law fits are shown as solid curves, and logarithmic fits are displayed as dashed curves.

for both periods showed that the ozone chemical lifetime was, indeed, long enough for the passive scalar assumption to be valid for our data, and that the difference in ζ_1 between the UT and LS was due to dynamical, not chemical lifetime, variation.

We have summarized the derived scaling parameters for the different subregions in Table 1. Note that there were not enough data below 30° latitude in the LS to make reliable calculations (the tropical tropopause is usually above cruising altitudes). Since these numbers were computed from fits and fits to fits, it was difficult to define a meaningful measure of uncertainty. Here the variations with respect to the regional subsets provide an idea of the stability of the parameters. We note that the differences between UT and LS parameters were greater than the regional differences within the UT or LS. In summary we can say that mesoscale isentropic ozone variability in the UT was rougher and more intermittent than in the LS. In the UT the equatorial ozone field was rougher than at higher latitudes, and the intermittency decreased with increasing absolute latitude. In the LS the intermittency and roughness were greater at high latitudes and over land than at midlatitudes and over the ocean.

In Figures 7 and 8 we compare the second-order structure functions of ozone with those of horizontal velocity and potential temperature in the UT and LS. For these calculations the data pairs were accepted if they were on the same standard flight level rather than on an isentropic surface (otherwise we would not have been able to compute the θ structure functions). The functional forms for ozone, however, were very similar to those presented in Figures 2 and 5. The point to be made with Figures 7 and 8 is that even though the veloc-

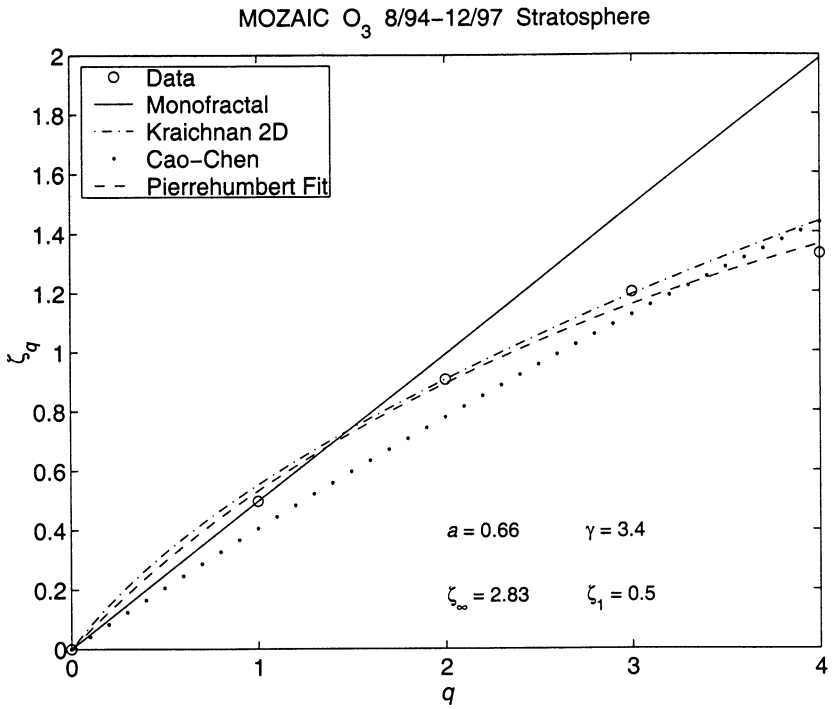

Figure 6. Plot of ζ_q calculated from the solid curves shown in Figure 5 (circles). Other functions are also plotted as indicated in the legend. See text for further details.

ity and potential temperature functions paralleled each other (except at the extreme short and long scales), the ozone S_2 were quite different in form throughout. The velocity second-order structure functions were investigated previously and were found to fit the form $Ar^{2/3} + Br^2 - Cr^2 \ln r$, where A, B, and C were fitting parameters, the first term corresponded to a $-5/3$ spectral power law (stratified turbulence or gravity wave cascade), and the last two terms corresponded to an enstrophy cascade 2-D turbulence subrange [*Lindborg*, 1999]. At mesoscales, regardless of whether the stratified turbulence or gravity wave cascade model is chosen, first-order advective ideas predict a tracer power spectrum (and S_2) of the same form as the velocity spectrum (and S_2) [*Gage and Nastrom*, 1986; *Bacmeister et al.*, 1996]. This kind of similarity is not observed here, especially in the LS, where $\beta = 1.9$ for ozone. At larger scales the tracer S_2 corresponding to 2-D enstrophy cascade turbulence should be logarithmic, and we have already seen that such a functional form cannot be fit to less than $r \sim 500$ km in the UT and $r \sim 100$ km in the LS, while the steep subrange of the velocity S_2 functions extend down to $r \sim 50$ km. Furthermore, we have already noted that the ozone structure functions did not follow simple scaling in this possibly logarithmic subrange; therefore large-scale ozone variability cannot be entirely attributed to smooth advection/diffusion.

Finally, we examine the issue of how the scaling pa-

Table 1. Ozone Scaling Parameters

Parameter	Latitude 0°–10°	10°–30°	30°–50°	50°–70°	Ocean	Land	All
			Troposphere, 2–256 km				
ζ_1	0.31	0.35	0.36	0.35	0.36	0.35	0.35
β	1.5	1.6	1.7	1.7	1.7	1.6	1.7
a	0.85	0.67	0.49	0.46	0.49	0.56	0.53
ζ_∞	0.7	1.1	2.2	2.3	2.3	1.4	1.6
			Stratosphere, 2–128 km				
ζ_1	...	...	0.52	0.49	0.51	0.48	0.50
β	...	...	2.0	1.9	1.9	1.9	1.9
a	...	...	0.62	0.67	0.63	0.68	0.66
ζ_∞	...	...	4.1	2.5	3.6	2.4	2.8

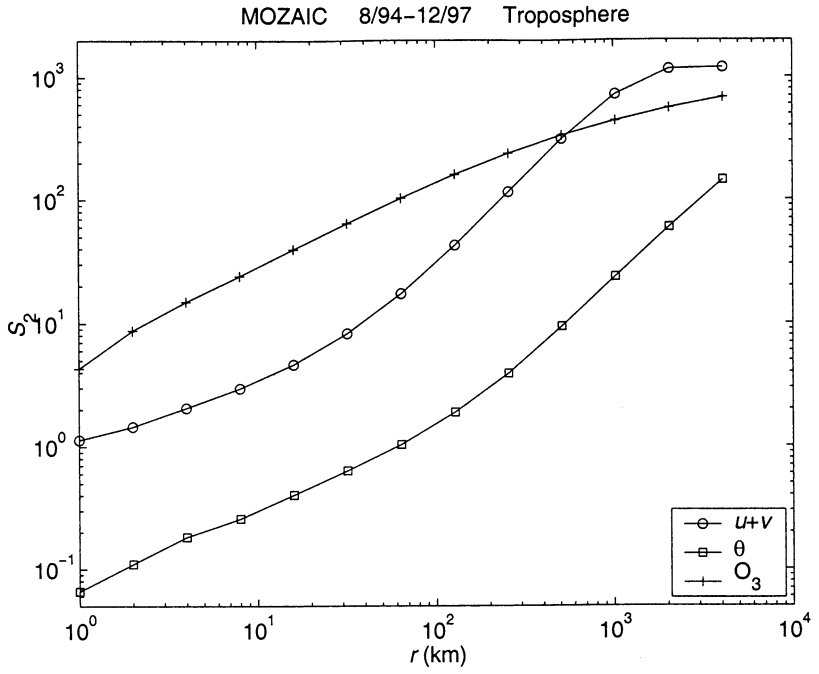

Figure 7. Plot of the sum of zonal and meridional wind S_2 (circles), potential temperature S_2 (squares), and ozone S_2 (crosses) for upper tropospheric data.

rameters differ between those calculated for averaged structure functions versus those computed for individual flights. Figure 9 displays histograms of ζ_1 and β calculated for each flight. Note that the mean, median, and mode values are very similar to the corresponding overall values in Table 1 for both the LS and UT. The distributions are well behaved in the sense that they are not far from Gaussian, and they provide a measure of the statistical uncertainties associated with the ζ_1 and β values in Table 1. These results give us additional confidence in the use of the averaged structure functions and that the differences between the LS and UT data are real. The transition zone (ozone concentration values between 100 and 200 ppbv) did not yield a long scaling interval ($r \sim$ 2–32 km) for the averaged structure functions, which was a reason why we did not include those results for our study. Even so, the transition zone results fall in between those of the LS and UT

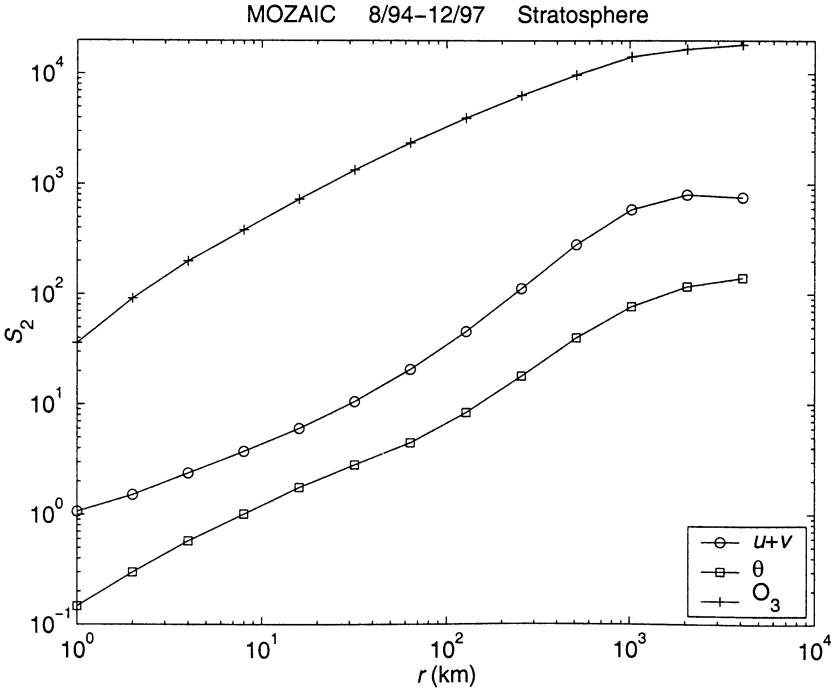

Figure 8. Same as Figure 7, except for lower stratospheric data.

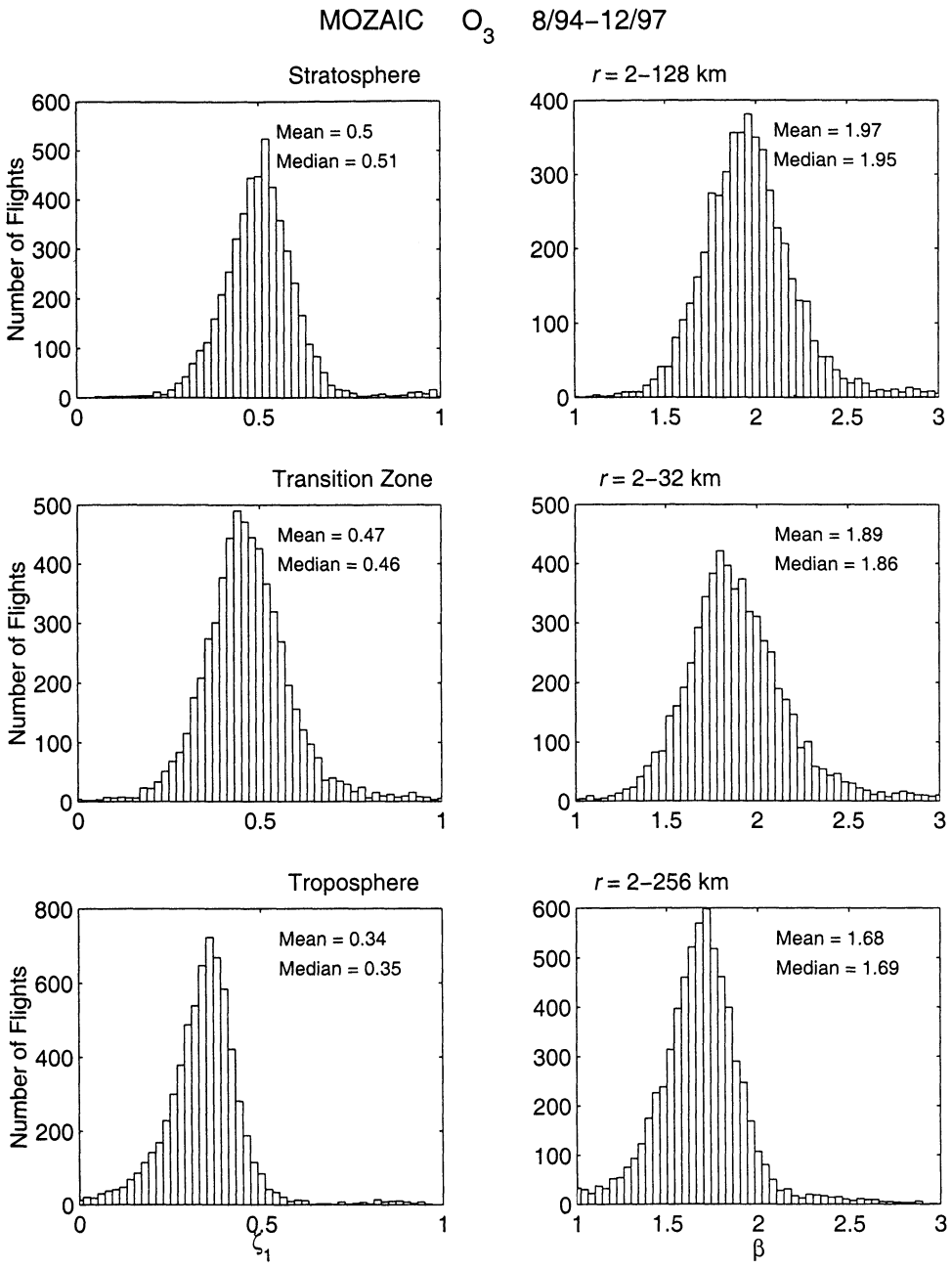

Figure 9. (top) Histograms of ζ_1 and β for the stratosphere, (middle) transition zone, i.e., ozone concentration values between 100 and 200 ppbv, and (bottom) troposphere.

as expected. Scaling parameters derived from higher-order structure functions were not computed because the scaling became poor in general for individual flights without the averaging process.

We also show the histograms for ζ_1 and β using all data, with and without the isentropic filter, in Figure 10. Clearly, the use of isentropic data pairs makes a difference in the results. With no isentropic requirement, $\beta = 2$, which is suggestive of square waves, i.e., an alternation of filaments or layers with different ozone concentrations. If ozone tended to maintain similar concentration levels along isentropic surfaces, then β could have been dominated by sudden transitions seen by the aircraft as it flew across the filaments. The use of the isentropic filter should have reduced the frequency of such transitions, thus also lowering the variance of the ozone concentration fluctuations, which was, in fact, evident (not shown here). The results here highlight the difficulty in comparing measured quantities (which are typically not along isentropes) and theories (which often rely on isentropic assumptions).

4. Increment PDFs

Although only in their infancy, theories for the increment (dissipation) PDF of passive scalar mixing have produced some predictions for specific cases. As with structure functions, PDFs are easy to compute, but

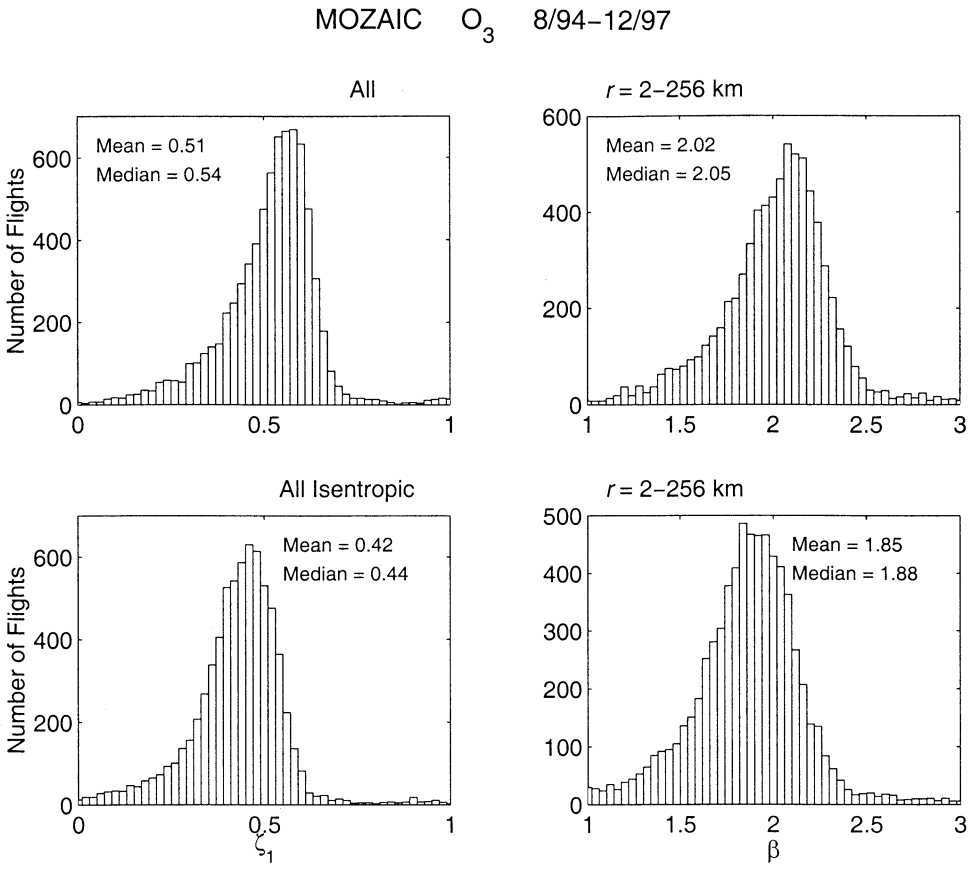

Figure 10. Histograms of ζ_1 and β for all data (top) with and (bottom) without the isentropic filter.

they can give us additional information about anomalously weak variability, which, for structure functions, require negative moments that usually lead to divergence.

Here we computed PDFs, $P(\Gamma)$, for $\Gamma = |\chi(x + r) - \chi(x)|^2/\sigma^2$, where σ was the standard deviation of the scalar difference. The calculation of r and the criteria used for isentropic data pairs and for discrimination between UT and LS data were the same as for the structure function calculations. Examples are shown in Figure 11, where $r = 4$ km. The functional forms were certainly not Gaussian, and attempts to fit the entire ranges to a lognormal dependency also yielded poor results. Stretched exponentials of the form, $P(\Gamma) \propto \exp(\eta\Gamma^\alpha)$, however, fit quite well and are shown as solid curves. The fitted parameters are displayed with subscript "t" for UT and "s" for LS data.

The variation of the PDFs with respect to r are summarized in Figures 12 and 13. The data point pair totals used for the PDFs were given in Figure 1. There is a smooth variation of the PDFs with r, which indicates anomalous scaling at all scales, a result we have already observed with the structure function analyses. The LS PDFs, however, collapse better to a single curve for $\Gamma \gtrsim 1$, which is also consistent with LS structure functions being closer to simple scaling than UT structure functions. As for regional variations, the tropical UT PDFs yielded poorer fits to the stretched exponential at the shortest scales, with a dip in the curves around $\Gamma \sim 1$.

Although the stretched exponential form fit the LS PDFs well for all r, it failed to fit the UT PDFs well for $r \geq 16$ km. With this caveat in mind we show the fitted α and η versus r in Figures 14 and 15. One should thus ignore UT data points for $r \geq 16$ km. Again, we see that the PDFs were continuously scale-dependent with no asymptotic behavior that might signal a simple-scaling range [*Vainshtein et al.*, 1994]. Values of α have been theoretically determined for a smooth, 2-D flow δ correlated in time ($\alpha = 1/3$ [*Chertkov et al.*, 1998]) and numerically modeled for the Batchelor regime ($\alpha = 0.3$–0.36 [*Holzer and Siggia*, 1994], $\alpha = 0.39$ [*Pierrehumbert*, 2000]). Our results fall in these ranges for $r \sim 30$–200 km in the LS. We also examined the percentage of $P(\Gamma > 1)$ for each PDF to see if there was an obvious transition point with respect to r that might indicate a dissipation scale, but we found none.

5. Summary Discussion

The main result of this study was that isentropic ozone variability in the UT/LS region scaled anomalously, even for large r, where there is strong evidence for an underlying smooth ($\beta \approx 3$) velocity field. We

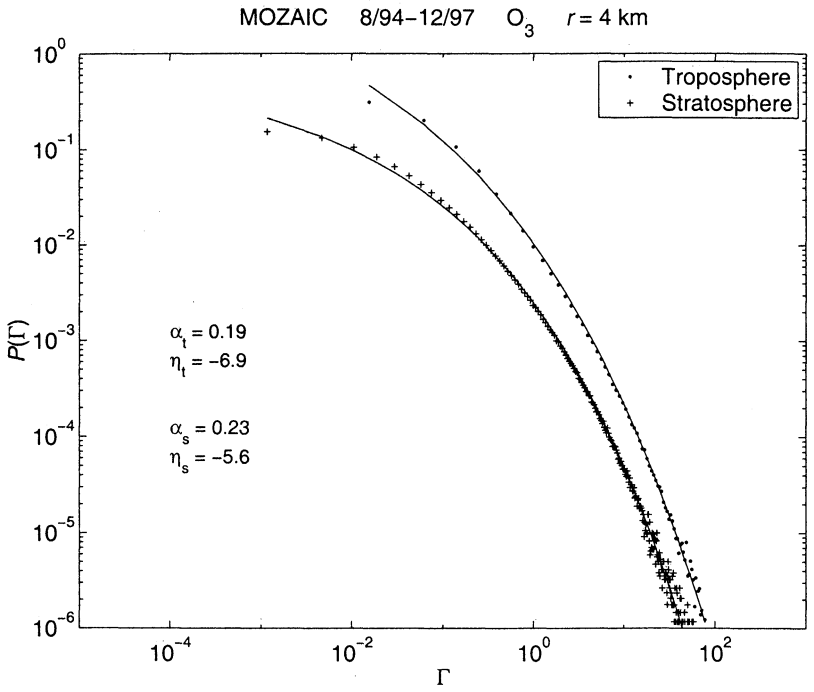

Figure 11. PDFs of Γ with $r = 4$ km. The solid curves are nonlinear least squares fits to a stretched exponential.

found no support for the simple scaling predicted for smooth advection/diffusion in the Batchelor regime. At mesoscales, ζ_q was more multifractal than the predictions for advection/diffusion by a 2-D random Gaussian velocity field δ correlated in time with self-similar correlations in space and was ill fit by a 3-D passive-scalar turbulence scheme based on a bivariate log-Poisson model. For UT data, ζ_q reached saturation for $q \gtrsim 5$. *Frisch et al.* [1999] have argued that saturation has general validity, even though the orders where it can be observed may be too high, depending on the spatial dimension and the roughness of the velocity field.

The lack of continuous scaling differs from the results of *Tuck and Hovde* [1999], who concluded that single-

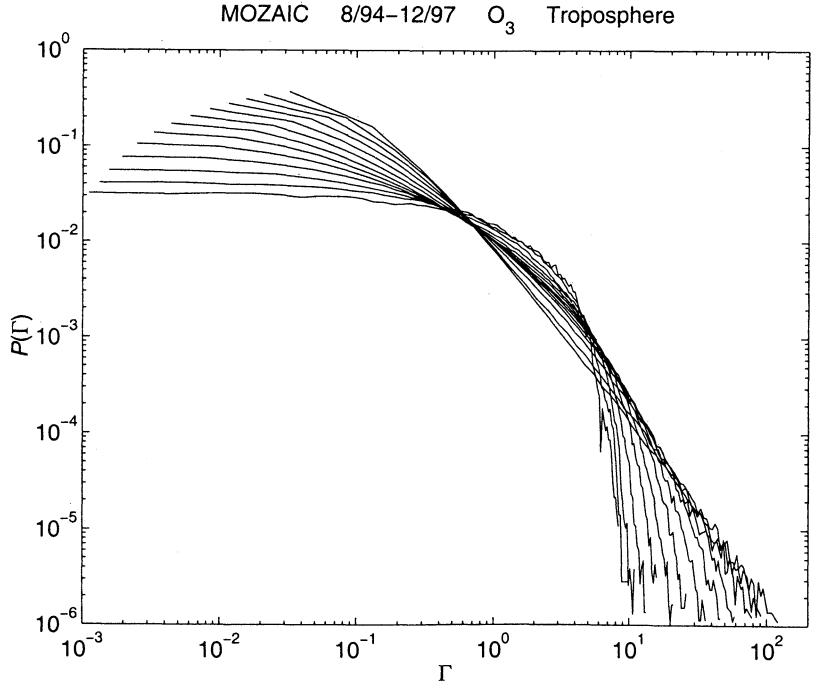

Figure 12. Upper tropospheric PDFs of Γ for r = 1–4096 km (from top to bottom at the small Γ end).

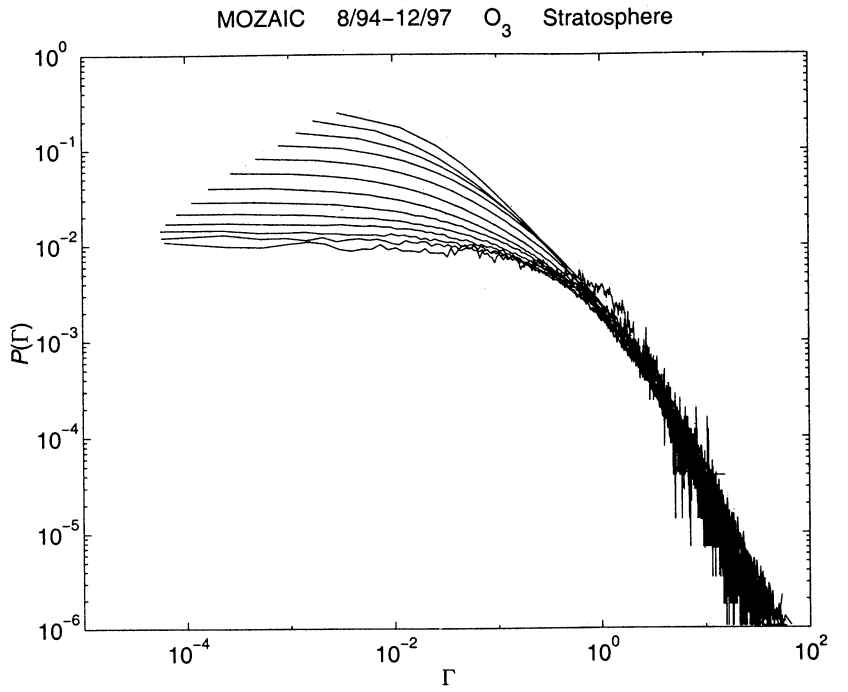

Figure 13. Lower stratospheric PDFs of Γ for r = 1–4096 km (from top to bottom at the small Γ end).

exponent scaling for ozone in the LS extends over 4 orders of magnitude up to one Earth radius. The difference may be due to the difference in approaches used. For example, *Vassilicos and Hunt* [1991] conclude that the scaling range can be more apparent with the Kolmogorov capacity than with spectral or autocorrelation methods. Another concern is the validity of Taylor's hypothesis at scales as long as an Earth radius. For velocity structure functions, there are indications that Taylor's hypothesis may be problematic for $r \gtrsim 1000$ km [*Lindborg*, 1999]. Also, the longer the time interval is between data points, the more likely it is for the passive scalar assumption for ozone to break down. In the UT, ozone precursors raised up by convection can speed up

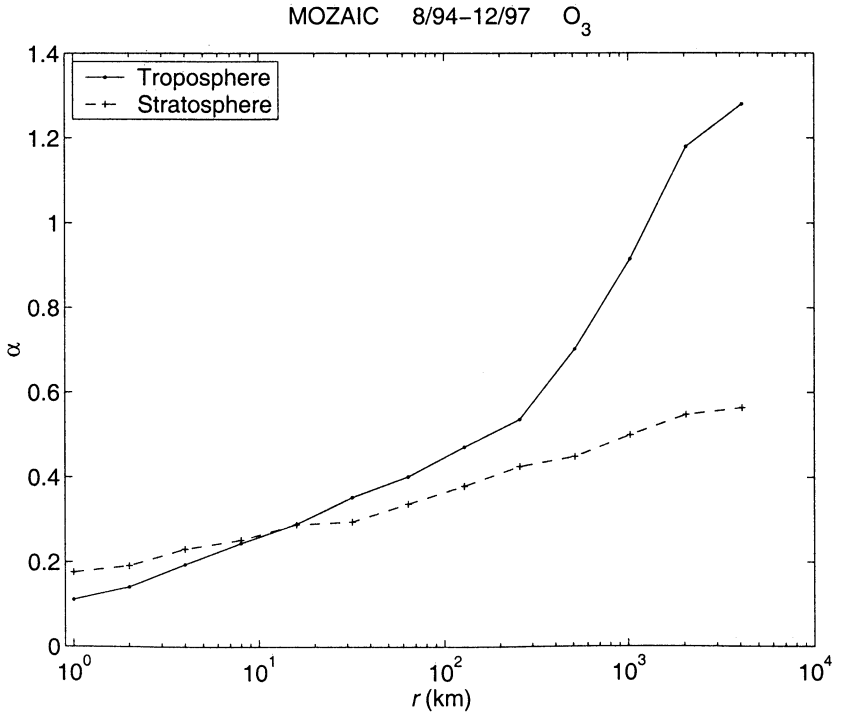

Figure 14. Plots of α versus r.

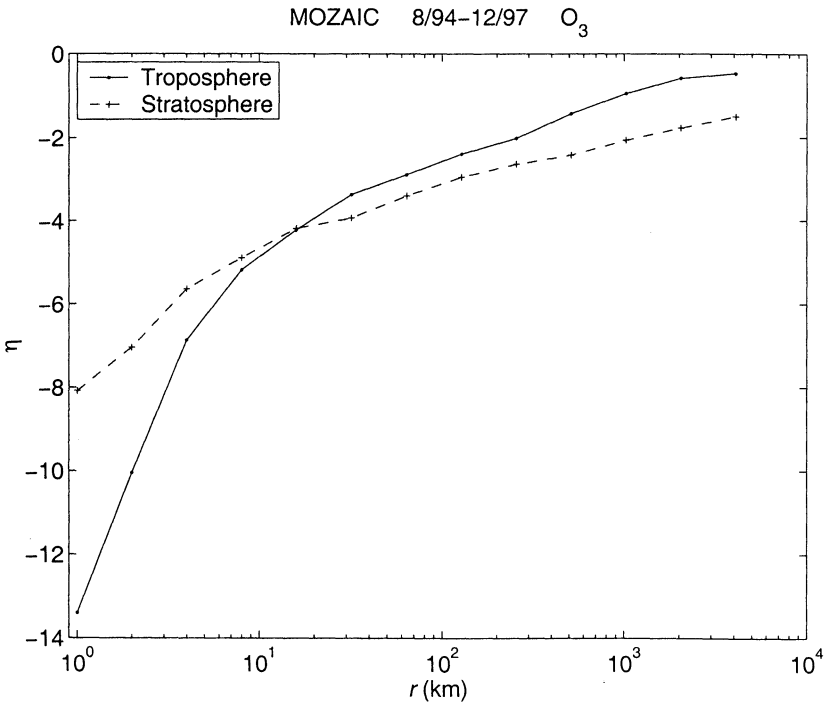

Figure 15. Plots of η versus r.

ozone production, while in the LS, chemically disturbed polar vortex air may extend to midlatitudes.

Isentropic increment PDFs for ozone were well fit by a stretched exponential function at all scales for LS data and for $r \lesssim 16$ km for UT data. However, the dependence of the fitting parameters on r showed again anomalous scaling throughout. Although instrumental response time limited this investigation to scales longer than ~2 km, our previous study using 20-Hz sampled water vapor data in the troposphere revealed anomalous scaling down to $r \sim 50$ m [*Cho et al.*, 2000], so it would not be surprising if ozone variability also scaled anomalously down to such short scales.

Regarding the differences between the UT and LS data, at mesoscales, UT ozone was rougher and more intermittent than LS ozone. This was probably due to perturbative features such as convective plumes that were present below the tropopause, which transported air across isentropes. Supporting this argument was the higher intermittency for UT at lower latitudes and over land regions, where convection should have been more vigorous than at higher latitudes and over the ocean. In the LS the intermittency and roughness were stronger at high latitudes and over land than at midlatitudes and over the ocean. This difference may be attributed to polar vortex effects at high latitudes and gravity waves that are preferentially generated over land by orographic forcing, which can then propagate upward through the tropopause [e.g., *Jasperson et al.*, 1990].

At large scales the concavity of the structure functions (especially for the LS data) suggested a possibly logarithmic dependency associated with a Batchelor regime, but as stated earlier, the scaling was anomalous (more so in the UT than in the LS). This result has implications for the use of contour advection [*Waugh and Plumb*, 1994; *Norton*, 1994], proven to work well in the stratosphere, which may seriously underestimate intermittency in the troposphere. It would be of interest to perform a scaling analysis on tracer variability produced by contour advection.

The basic problem we face at this point is the lack of theoretical predictions for realistic conditions. Much of the initial work in this field has been focused on 3-D inertial range turbulence, while the dynamics of the atmosphere at these scales consist of quasi-2-D turbulence, 3-D waves, and convective motions. Clearly, models have the most difficulty properly representing vertical and cross-isentropic advection, and this is going to be a continuing challenge in the future. In the troposphere, chemical transport models without convection will not obtain accurate results in general. The degree of intermittency may become an important parameter in determining the amount of convection that needs to be included in such models in the future.

Acknowledgments. The work at MIT was supported by NASA grant NAG1-2306. MOZAIC was funded in part by the European Communities (DG XII-C, DG XII-D) with strong support from Airbus Industrie and its partners, Air France, Lufthansa, Austrian Airlines, and Sabena. J.Y.N.C. would also like to thank Erik Lindborg, Ray Pierrehumbert, and Lynn Sparling for helpful discussions.

References

Antonsen, T. M., Z. Fan, E. Ott, and E. Garcia-Lopez, The role of chaotic orbits in the determination of power spectra of passive scalars, *Phys. Fluids*, *8*, 3094–3104, 1996.

Bacmeister, J. T., S. D. Eckermann, P. A. Newman, L. Lait, K. R. Chan, M. Loewenstein, M. H. Proffitt, and B. L. Gary, Stratospheric horizontal wavenumber spectra of winds, potential temperature, and atmospheric tracers observed by high-altitude aircraft, *J. Geophys. Res.*, *101*, 9441–9470, 1996.

Bacmeister, J. T., S. D. Eckermann, L. Sparling, K. R. Chan, M. Loewenstein, and M. H. Proffitt, Analysis of intermittency in aircraft measurements of velocity, temperature and atmospheric tracers using wavelet transforms, in *Gravity Wave Processes: Their Parameterization in Global Climate Models, NATO ASI Ser., Ser. I, vol. 50*, edited by K. Hamilton, pp. 85–102, Springer-Verlag, New York, 1997.

Balkovsky, E., and V. Lebedev, Instanton for the Kraichnan random advection model, *Phys. Rev. E Stat. Phys. Plasmas Fluids Relat. Interdiscip. Top.*, *58*, 5776–5795, 1998.

Batchelor, G. K., Small-scale variation of convected quantities like temperature in a turbulent fluid, part 1, *J. Fluid Mech.*, *5*, 113–133, 1959.

Brasseur, G. P., J. J. Orlando, and G. S. Tyndall, *Atmospheric Chemistry and Global Change*, 654 pp., Oxford Univ. Press, New York, 1999.

Cao, N., and S. Chen, An intermittency model for passive-scalar turbulence, *Phys. Fluids*, *9*, 1203–1205, 1997.

Chertkov, M., Instanton for random advection, *Phys. Rev. E Stat. Phys. Plasmas Fluids Relat. Interdiscip. Top.*, *55*, 2722–2735, 1997.

Chertkov, M., G. Falkovich, I. Kolokolov, and I. Lebedev, Statistics of a passive scalar advected by a large-scale two-dimensional velocity field: Analytic solution, *Phys. Rev. E Stat. Phys. Plasmas Fluids Relat. Interdiscip. Top.*, *51*, 5609–5627, 1995.

Chertkov, M., G. Falkovich, and I. Kolokolov, Intermittent dissipation of a passive scalar in turbulence, *Phys. Rev. Lett.*, *80*, 2121–2124, 1998.

Cho, J. Y. N., and E. Lindborg, Horizontal velocity structure functions in the upper troposphere and lower stratosphere, 1, Observations, *J. Geophys. Res.*, in press, 2001.

Cho, J. Y. N., R. E. Newell, and J. D. Barrick, Horizontal wavenumber spectra of winds, temperature, and trace gases during the Pacific Exploratory Missions, 2, Gravity waves, quasi-two-dimensional turbulence, and vortical modes, *J. Geophys. Res.*, *104*, 16,297–16,308, 1999a.

Cho, J. Y. N., R. E. Newell, V. Thouret, A. Marenco, and H. G. Smit, Trace gas study accumulates forty million frequent-flyer miles for science, *Eos Trans. AGU*, *80*, 377, 383–384, 1999b.

Cho, J. Y. N., Y. Zhu, R. E. Newell, B. E. Anderson, J. D. Barrick, G. L. Gregory, G. W. Sachse, M. A. Carroll, and G. M. Albercook, Horizontal wavenumber spectra of winds, temperature, and trace gases during the Pacific Exploratory Missions, 1, Climatology, *J. Geophys. Res.*, *104*, 5697–5716, 1999c.

Cho, J. Y. N., R. E. Newell, and G. W. Sachse, Anomalous scaling of mesoscale tropospheric humidity fluctuations, *Geophys. Res. Lett.*, *27*, 377–380, 2000.

Davis, A., A. Marshak, W. Wiscombe, and R. Cahalan, Multifractal characterizations of nonstationarity and intermittency in geophysical fields: Observed, retrieved, or simulated, *J. Geophys. Res.*, *99*, 8055–8072, 1994.

Davis, A. B., A. Marshak, R. F. Cahalan, and W. J. Wiscombe, Interactions: Solar and laser beams in stratus clouds, fractals and multifractals in climate and remote sensing studies, *Fractals*, *5*, 129–166, 1997.

Davis, A. B., A. Marshak, H. Gerber, and W. J. Wiscombe, Horizontal structure of marine boundary layer clouds from centimeter to kilometer scales, *J. Geophys. Res.*, *104*, 6123–6144, 1999.

Dewan, E. M., Stratospheric wave spectra resembling turbulence, *Science*, *204*, 832–835, 1979.

Dewan, E. M., and N. Grossbard, Power spectral artifacts in published balloon data and implications regarding saturated gravity wave theories, *J. Geophys. Res.*, *105*, 4667–4684, 2000.

Fasham, M. J. R., The statistical and mathematical analysis of plankton patchiness, *Oceanogr. Mar. Biol.*, *16*, 43–79, 1978.

Frisch, U., From global scaling à la Kolmogorov, to local multifractal in fully developed turbulence, *Proc. R. Soc. London, Ser. A*, *434*, 89–99, 1991.

Frisch, U., *Turbulence: The Legacy of A. N. Kolmogorov*, 296 pp., Cambridge Univ. Press, New York, 1995.

Frisch, U., A. Mazzino, and M. Vergassola, Lagrangian dynamics and high-order moments intermittency in passive scalar advection, *Phys. Chem. Earth B*, *24*, 945–951, 1999.

Gage, K. S., Evidence for a $k^{-5/3}$ law inertial range in mesoscale two-dimensional turbulence, *J. Atmos. Sci.*, *36*, 1950–1954, 1979.

Gage, K. S., and G. D. Nastrom, Spectrum of atmospheric vertical displacements and spectrum of conservative scalar passive additives due to quasi-horizontal atmospheric motions, *J. Geophys. Res.*, *91*, 13,211–13,216, 1986.

Gardner, C. S., C. A. Hostetler, and S. Lintelman, Influence of the mean wind field on the separability of atmospheric perturbation spectra, *J. Geophys. Res.*, *98*, 8859–8872, 1993.

Helten, M., H. G. J. Smit, W. Sträter, D. Kley, P. Nédélec, M. Zöger, and R. Busen, Calibration and performance of automatic compact instrumentation for the measurement of relative humidity from passenger aircraft, *J. Geophys. Res.*, *103*, 25,643–25,652, 1998.

Holzer, M., and E. D. Siggia, Turbulent mixing of a passive scalar, *Phys. Fluids*, *6*, 1820–1837, 1994.

Jasperson, W. H., G. D. Nastrom, and D. C. Fritts, Further study of terrain effects on the mesoscale spectrum of atmospheric motions, *J. Atmos. Sci.*, *47*, 979–987, 1990.

Kraichnan, R., Anomalous scaling of a randomly advected passive scalar, *Phys. Rev. Lett.*, *72*, 1016–1019, 1994.

Lesieur, M., J. Sommeria, and G. Holloway, Inertial ranges of the spectrum of a passive contaminant in two-dimensional turbulence, *C. R. Seances Acad. Sci., Ser. B*, *292*, 271–274, 1981.

Lilly, D. K., Stratified turbulence and the mesoscale variability of the atmosphere, *J. Atmos. Sci.*, *40*, 749–761, 1983.

Lilly, D. K., Two-dimensional turbulence generated by energy sources at two scales, *J. Atmos. Sci.*, *46*, 2026–2030, 1989.

Lindborg, E., Can the atmospheric kinetic energy spectrum be explained by two-dimensional turbulence?, *J. Fluid Mech.*, *388*, 259–288, 1999.

Lindborg, E., and J. Y. N. Cho, Determining the cascade of passive scalar variance in the lower stratosphere, *Phys. Rev. Lett.*, *85*, 5663–5666, 2000.

Lindborg, E., and J. Y. N. Cho, Horizontal velocity structure functions in the upper troposphere and lower stratosphere, 2, Theoretical considerations, *J. Geophys. Res.*, in press, 2001.

Marenco, A., *MOZAIC I, Measurement of Ozone by Airbus In-Service Aircraft: Technical Final Report, 1993–1996*, 276 pp., Université Paul Sabatier, Toulouse, France, 1996.

Marenco, A., et al., Measurement of ozone and water vapor by Airbus in-service aircraft: The MOZAIC airborne program, An overview, *J. Geophys. Res.*, *103*, 25,631–25,642, 1998.

Marshak, A., A. Davis, R. Cahalan, and W. Wiscombe, Bounded cascade models as nonstationary multifractals,

Phys. Rev. E Stat. Phys. Plasmas Fluids Relat. Interdiscip. Top., *49*, 55–69, 1994.

Methven, J., and B. Hoskins, Spirals in potential vorticity, part I, Measures of structure, *J. Atmos. Sci.*, *55*, 2053–2066, 1998.

Nastrom, G. D., and K. S. Gage, A climatology of atmospheric wavenumber spectra of wind and temperature observed by commercial aircraft, *J. Atmos. Sci.*, *42*, 950–960, 1985.

Nastrom, G. D., W. H. Jasperson, and K. S. Gage, Horizontal spectra of atmospheric tracers measured during the Global Atmospheric Sampling Program, *J. Geophys. Res.*, *91*, 13,201–13,209, 1986.

Norton, W. A., Breaking Rossby waves in a model stratosphere diagnosed by a vortex-following coordinate system and a technique for advecting material contours, *J. Atmos. Sci.*, *51*, 654–673, 1994.

Pierrehumbert, R. T., On tracer microstructure in the large-eddy dominated regime, *Chaos Solitons Fractals*, *4*, 1091–1110, 1994.

Pierrehumbert, R. T., Anomalous scaling of high cloud variability in the tropical Pacific, *Geophys. Res. Lett.*, *23*, 1095–1098, 1996.

Pierrehumbert, R. T., Lattice models of advection-diffusion, *Chaos*, *10*, 61–74, 2000.

Shraiman, B. I., and E. D. Siggia, Scalar turbulence, *Nature*, *405*, 639–646, 2000.

Sparling, L. C., J. A. Kettleborough, P. H. Haynes, M. E. McIntyre, J. E. Rosenfield, M. R. Schoeberl, and P. A. Newman, Diabatic cross-isentropic dispersion in the lower stratosphere, *J. Geophys. Res.*, *102*, 25,817–25,829, 1997.

Tessier, Y., S. Lovejoy, and D. Schertzer, Universal multifractals: Theory and observations for rain and clouds, *J. Appl. Meteorol.*, *32*, 223–250, 1993.

Thouret, V., A. Marenco, P. Nédélec, and C. Grouhel, Ozone climatologies at 9–12 km altitude as seen by the MOZAIC airborne program between September 1994 and August 1996, *J. Geophys. Res.*, *103*, 25,653–25,679, 1998.

Tuck, A. F., and S. J. Hovde, Fractal behavior of ozone, wind and temperature in the lower stratosphere, *Geophys. Res. Lett.*, *26*, 1271–1274, 1999.

Tuck, A. F., S. J. Hovde, and M. H. Proffitt, Persistence in ozone scaling under the Hurst exponent as an indicator of the relative rates of chemistry and fluid mechanical mixing in the stratosphere, *J. Phys. Chem. A*, *103*, 10,445–10,450, 1999.

Vainshtein, S. I., K. R. Sreenivasan, R. T. Pierrehumbert, V. Kashyap, and A. Juneja, Scaling exponents for turbulence and other random-processes and their relationships with multifractal structure, *Phys. Rev. E*, *50*, 1823–1835, 1994.

VanZandt, T. E., A universal spectrum of buoyancy waves in the atmosphere, *Geophys. Res. Lett.*, *9*, 575–578, 1982.

Vassilicos, J. C., and J. C. R. Hunt, Fractal dimensions and spectra of interfaces with application to turbulence, *Proc. R. Soc. London, Ser. A*, *435*, 505–534, 1991.

Wang, Y., D. J. Jacob, and J. A. Logan, Global simulation of tropospheric O_3-NO_x-hydrocarbon chemistry, 3, Origin of tropospheric ozone and effects of nonmethane hydrocarbons, *J. Geophys. Res.*, *103*, 10,757–10,767, 1998.

Waugh, D. W., and R. A. Plumb, Contour advection with surgery: A technique for investigating fine-scale structure in tracer transport, *J. Atmos. Sci.*, *51*, 530–540, 1994.

J. Y. N. Cho and R. E. Newell, Department of Earth, Atmospheric, and Planetary Sciences, Massachusetts Institute of Technology, 77 Massachusetts Ave., Rm. 54-1823, Cambridge, MA 02139-4307. (jcho@pemtropics.mit.edu; renewell@mit.edu)

A. Marenco and V. Thouret, Laboratoire d'Aérologie, CNRS (UMR 5560), OMP, UPS, 14 Avenue Edouard Belin, 31400 Toulouse, France. (mara@aero.obs-mip.fr; thov@aero.obs-mip.fr)

(Received April 6, 2000; revised August 30, 2000; accepted October 18, 2000.)